REPORT DOCUMENTATION PAGE

Form Approved OMB NO. 0704-0188

1. REPORT DATE (DD-MM-YYYY)	2. REPORT TYPE	3. DATES COVERED (From - To)
17-03-2015	Final Report	18-Apr-2011 - 17-Dec-2014

4. TITLE AND SUBTITLE
Final Report: Portable Sensor for Detecting Microbubbles in Real Time to Prevent Decompression Sickness for Safe Diving During Subaquatic Navy Activities

5a. CONTRACT NUMBER
W911NF-11-1-0135

5b. GRANT NUMBER

5c. PROGRAM ELEMENT NUMBER
206022

6. AUTHORS
Silvina Cancelos

5d. PROJECT NUMBER

5e. TASK NUMBER

5f. WORK UNIT NUMBER

7. PERFORMING ORGANIZATION NAMES AND ADDRESSES
University of Puerto Rico at Mayaguez
R & D Center
Call Box 9000
Mayaguez, PR 00681 -9000

8. PERFORMING ORGANIZATION REPORT NUMBER

9. SPONSORING/MONITORING AGENCY NAME(S) AND ADDRESS (ES)
U.S. Army Research Office
P.O. Box 12211
Research Triangle Park, NC 27709-2211

10. SPONSOR/MONITOR'S ACRONYM(S)
ARO

11. SPONSOR/MONITOR'S REPORT NUMBER(S)
59067-LS-REP.4

12. DISTRIBUTION AVAILIBILITY STATEMENT
Distribution authorized to U.S. Government Agencies Only, Contains Proprietary information

13. SUPPLEMENTARY NOTES
The views, opinions and/or findings contained in this report are those of the author(s) and should not contrued as an official Department of the Army position, policy or decision, unless so designated by other documentation.

14. ABSTRACT
The objective of this research project was to determine the feasibility of a new technology that would allow Navy divers to monitor in real time the presence, number and size of nitrogen bubbles, protecting them against DCS. We have successfully proven the feasibility of the idea. A system for generating air bubbles a small as 150um was developed. We were capable of detecting bubbles in the artificial blood vessels and in the artificial soft tissue. The electrical signals measured on the PZT were correlated to the size of the bubbles

15. SUBJECT TERMS
decompression sickness, bubble dynamics, bubble detection

16. SECURITY CLASSIFICATION OF:			17. LIMITATION OF ABSTRACT	15. NUMBER OF PAGES	19a. NAME OF RESPONSIBLE PERSON
a. REPORT	b. ABSTRACT	c. THIS PAGE			Silvina Cancelos
UL	UL	UL	UL		19b. TELEPHONE NUMBER 787-832-4040

Report Title

Final Report: Portable Sensor for Detecting Microbubbles in Real Time to Prevent Decompression Sickness for Safe Diving During Subaquatic Navy Activities

ABSTRACT

The objective of this research project was to determine the feasibility of a new technology that would allow Navy divers to monitor in real time the presence, number and size of nitrogen bubbles, protecting them against DCS. We have successfully proven the feasibility of the idea. A system for generating air bubbles a small as 150um was developed. We were capable of detecting bubbles in the artificial blood vessels and in the artificial soft tissue. The electrical signals measured on the PZT were correlated to the size of the bubbles

---

Enter List of papers submitted or published that acknowledge ARO support from the start of the project to the date of this printing. List the papers, including journal references, in the following categories:

(a) Papers published in peer-reviewed journals (N/A for none)

Received Paper

TOTAL:

Number of Papers published in peer-reviewed journals:

(b) Papers published in non-peer-reviewed journals (N/A for none)

Received Paper

TOTAL:

Number of Papers published in non peer-reviewed journals:

(c) Presentations

Number of Presentations: 0.00

Non Peer-Reviewed Conference Proceeding publications (other than abstracts):

Received	Paper	
08/27/2012	2.00	Francisco I Valentin, Silvina Cancelos. Detecting presence of bubbles within simulated blood vessels using a piezoelectric ring set to oscillate at matching resonant conditions, ASME 2012 Summer Bioengineering Conference. 20-JUN-12, . : ,
TOTAL:	**1**	

Number of Non Peer-Reviewed Conference Proceeding publications (other than abstracts):

Peer-Reviewed Conference Proceeding publications (other than abstracts):

Received	Paper	
08/27/2012	1.00	Francisco I. Valentin, Silvina Cancelos. Predicting bubble migration due to Bjerknes force in a complex 3D geometry, ASME Fluids Engineering Summer Meeting. 08-JUL-12, . : ,
TOTAL:	**1**	

Number of Peer-Reviewed Conference Proceeding publications (other than abstracts):

(d) Manuscripts

Received	Paper
TOTAL:	

Number of Manuscripts:

Books

Received Book

TOTAL:

Received Book Chapter

TOTAL:

Patents Submitted

Personal, real time sensor to monitor amount and size of bubbles in the bloodstream and/or tissues

(Note: a provisional patent was submitted)

Patents Awarded

Awards

Graduate Students

NAME	PERCENT_SUPPORTED	Discipline
Andres Saavedra	0.44	
William Garcia	0.37	
Armando Figueroa	0.03	
Angel Camelo	0.03	
Emanuel Torres	0.01	
Francisco Valentin	0.00	
FTE Equivalent:	**0.88**	
Total Number:	**6**	

Names of Post Doctorates

NAME	PERCENT_SUPPORTED
FTE Equivalent:	
Total Number:	

Names of Faculty Supported

NAME	PERCENT_SUPPORTED	National Academy Member
Silvina Cancelos	0.15	
Carlos Marin	0.05	
FTE Equivalent:	**0.20**	
Total Number:	**2**	

Names of Under Graduate students supported

NAME	PERCENT_SUPPORTED	Discipline
Jesus Banchs	0.03	Mechanical Engineering
Yesed Sanchez	0.03	Mechanical Engineering
Ahmed Perez Lugo	0.12	Mechanical Engineering
Luis Sanchez Fuentes	0.07	Mechanical Engineering
Orniz Quiñones	0.03	Mechanical Engineering
Joshua Aponte	0.03	Mechanical Engineering
Gabriel Villamizar	0.12	Mechanical Engineering
Carlos Poventud	0.03	Chemical Engineering
Taniushka Tomas Valeriano	0.09	Mechanical Engineering
FTE Equivalent:	**0.55**	
Total Number:	**9**	

Student Metrics

This section only applies to graduating undergraduates supported by this agreement in this reporting period

The number of undergraduates funded by this agreement who graduated during this period: 7.00

The number of undergraduates funded by this agreement who graduated during this period with a degree in science, mathematics, engineering, or technology fields:..... 7.00

The number of undergraduates funded by your agreement who graduated during this period and will continue to pursue a graduate or Ph.D. degree in science, mathematics, engineering, or technology fields:..... 3.00

Number of graduating undergraduates who achieved a 3.5 GPA to 4.0 (4.0 max scale):..... 4.00

Number of graduating undergraduates funded by a DoD funded Center of Excellence grant for Education, Research and Engineering:..... 0.00

The number of undergraduates funded by your agreement who graduated during this period and intend to work for the Department of Defense 0.00

The number of undergraduates funded by your agreement who graduated during this period and will receive scholarships or fellowships for further studies in science, mathematics, engineering or technology fields:..... 1.00

Names of Personnel receiving masters degrees

NAME
Francisco Valentin
Total Number: 1

Names of personnel receiving PHDs

NAME

Total Number:

Names of other research staff

NAME PERCENT_SUPPORTED

FTE Equivalent:
Total Number:

Sub Contractors (DD882)

Inventions (DD882)

5 **"Personal, real time sensor to monitor amount and size of bubbles in the bloodstream and/or tissues"**

Patent Filed in US? (5d-1) Y
Patent Filed in Foreign Countries? (5d-2) N
Was the assignment forwarded to the contracting officer? (5e) N
Foreign Countries of application (5g-2):

5a: Silvina Cancelos
5f-1a: University of Puerto Rico - Mayaguez
5f-c: CALL BOX 9000
Mayaguez PR 00681

5a: Andres Saavedra
5f-1a: University of Puerto Rico - Mayaguez
5f-c: CALL BOX 9000
MAYAGUEZ PR 00681

5a: Francisco Valentin
5f-1a:
5f-c:

5a: Carlos Marin
5f-1a: University of Puerto Rico - Mayaguez
5f-c: CALL BOX 9000
MAYAGUEZ PR 00681

Scientific Progress

Technology Transfer

UNIVERSITY OF PUERTO RICO - MAYAGUEZ

Portable Sensor for Detecting Microbubbles in Real Time to Prevent Decompression Sickness for Safe Diving During Subaquatic Navy Activities

Final Report
Scientific Progress and Accomplishments

Contract# W911NF-11-1-0135
Proposal# 59067-LS-REP

Silvina Cancelos, Ph.D

3/17/2015

Table of Contents

1 Introduction

Humans developing activities in conditions requiring significant change in the ambient pressure might nucleate nitrogen bubbles in tissues and/or bloodstream. These bubbles are known to precede decompression sickness (DCS) symptoms. Currently, divers rely on decompression tables which are designed to decrease the incidence of DCS. Since the tables are based on reducing the statistical risk for an individual based on a population-based norm, there is no safe approach to individualize preventive measures. Thus, a diver may have to undergo several hours of decompression that might be unnecessary. This annoyance becomes more salient when divers do not have access to a recompression chamber and have to undergo in water recompression. This significantly increases the risk to the divers, especially in conditions of turbulent sea state or combat scenarios. Despite over a century of dealing with DCS, decompression tables remain the standard operation protocol for surfacing. Nevertheless, it is striking the fact that 85% of reported DCS cases occur to divers who follow decompression tables and who did not develop DCS symptoms during previous immersions following identical protocols.

2 Statement of the problem studied

Currently, bubbles may be detected using Doppler ultrasound. However, Doppler has several disadvantages as a detection technique in that (i) Doppler is sensitive to motion, (ii) bubbles have to be greater than 80 μm in diameter to be detected and (iii) detection systems cannot be miniaturized in portable/personal devices. Additionally, it has been shown that the levels of decompression typically undergone by humans during diving are not enough to spontaneously nucleate nitrogen bubbles; therefore, it has been hypothesized, that gas nuclei must exist in blood and tissue in order to initiate bubble formation and growth (Harvey 1940 and Hempleman 1993). Recently, a group of researchers from Dartmouth Medical School and Creare, Inc., made important advances that can lead to a better understanding on the mechanisms of bubble formation during decompression and to protocols that could predict the risk of DCS by detecting pre-existing micronuclei non-invasively before commencing sub-aquatic activities (Bollinger et al., 2009).

However, there is a lack of technologies able to produce personal/portable devices for continuous monitoring of bubble presence in the bloodstream. The objective of this research project is to determine the feasibility of a new technology proposed by the PI that would make possible fabrication of such devices.

3 Summary of the most important results related to the proposed tasks described in the proposal

- Task #1: A simplified artificial thigh was modelled and numerical results obtained using COMSOL Multiphysics. Acoustic pressure distribution and Bjerknes force were obtained and compared to experimental results obtaining excellent agreement.

- Task #2: The third generation of artificial thigh was constructed and the design was proven to be robust having the same behavior in terms of electrical admittance over time.

- Task #3: Two high speed cameras with two LED lights were synchronized with the acquisition of electrical signals from the PZT and microphones through a USB timing HUB, allowing us to correlate bubble size and electric signal.

- Task #4: Even though 4 methods for creating bubbles were originally proposed, we have only worked with one, since it was the only method in which air bubbles were produced. The other methods could generate smaller bubbles but with a high content of vapor and thus a different dynamics. The smallest bubbles we produced in a control manner have a 50μm in radius. Advances were made in order to generate smaller air bubbles, the necessary equipment was purchased and installed, but unfortunately we could not yet test it.

- Task #5: The bubble generation device was successfully integrated in the artificial thigh system, producing repeatable results.

- Task #6: A LabView code was developed to obtain electric signals from the PZT (current, voltage and phase) as well as the voltage from 3 pill microphones.

- Task #7: A total of 126 experiments were conducted under comparable conditions using the 3rd generation of artificial thigh and the method 2 for measuring the current on the PZT. These experiments measured the transient response in the PZT when the PZT is actuated when the bubble crosses the PZT center. Some experiments were conducted with water, others with hyaluronic acid at 0.66% and with hyaluronic acid at 1.05%. Also, 38 of these experiments also monitored the signal of 3 pill microphones. 25 additional experiments were conducted actuating the PZT when the bubbles were 1cm away from the PZT. 20 experiments more were carried when the bubble was at 2cm of the PZT, this later case showed that the current in the PZT did not change, therefore, the system is not capable of detecting bubbles when they are 2cm away from the PZT or more.

- Task #8 Even though the design of the bubble generator for introducing 3 bubbles of same size was finalized, it could not be constructed. Therefore tests were not conducted.

- Task #9 Since the project was extended only for 8 months, it was decided not to pursue this task.

- Task #10 This task was conducted in a slightly different manner as to what it was originally proposed. The hyaluronic acid was degassed prior to filling and bubbles were introduced in a controlled manner in the soft tissue and successfully detected by the PZT. 7 experiments were conducted with bubbles ranging from 250um to 2000um. The same technique applied to bubbles in the artery was successfully used in detecting the bubbles in the soft tissue.

- Task #11 An algorithm capable of predicting the size of the bubble crossing the PZT was successfully implemented. Neural network algorithm has proven to be the most effective when the signals of the microphone are used in combination with the percentage of the difference in root mean square of the voltage in the PZT.

- Task #12 Since the project was extended only for 8 months, it was decided not to pursue this task.

Below we present some of the most relevant technical details.

3.1 Detailed work related to Task#1 and Task#2 (3D model and construction of the simplified artificial thigh)

Three generations of simplified artificial thigh were designed and constructed.

3.1.1 1st generation of artificial thigh

The first generation is well documented in the MS thesis of Valentín F. (2012) Chapter 3 Pages 54-64 and Chapter 4. This design consisted mainly of a glass cylinder with 95mm in outside diameter and 300mm height surrounded by a piezoelectric ring (BM400, Sensor Technology, Ontario, Canada) with 110mm outside diameter, 98mm inside diameter and 25mm in height. At the center of the glass cylinder a composite bone was located. The artificial bone is a cylinder with 20mm in outside diameter and 300mm in height and it is made of a short-fiber-filled epoxy filled with polyurethane foam (3403-21, Saw Bones, Vashon Island, Washington). Two flanges were incorporated in the design to hold the glass cylinder as well as the plastic tubing that will serve as the main femoral vein and artery. The material chosen for the flanges was acrylic because it has acoustic properties similar to those of glass. The glass cylinder, flanges and bone were glued using Blue Silicone RTV adhesive. The PZT was glued to the glass cylinder using epoxy Stycast 1264. A small PZT disk with 6mm in diameter (hereafter called pill microphone) was glued to the glass cylinder. The pill microphone is susceptible to bubble oscillations. All the fittings used in the design of the artificial thigh need to withstand vacuum pressures of 0.1 Torr. Swagelok was chosen as the provider of these fittings. Figure 1 shows a schematic as well as the as-built 1st generation of artificial thigh. Figure 2 shows the connections used to vacuum the inside of the cylinder prior to fill it with deionized (Millipore Simplicity SIMS 6000 Type 1) and degassed water. The integration of the bubble generation device in the loop is also shown in Figure 2. A 3D

numerical model of this design was performed. Details of the numerical simulation can be found in the MS thesis of Valentín F. (2012). With the results obtained from the numerical simulations, the Bjerknes force was computed and prediction of the bubble migration patterns was possible, allowing us to improve the detection techniques.

The research performed with the 1st generation of artificial thigh allowed us to conclude that the proposed system was capable of detecting bubbles and that the best quantity to measure was the current on the PZT.

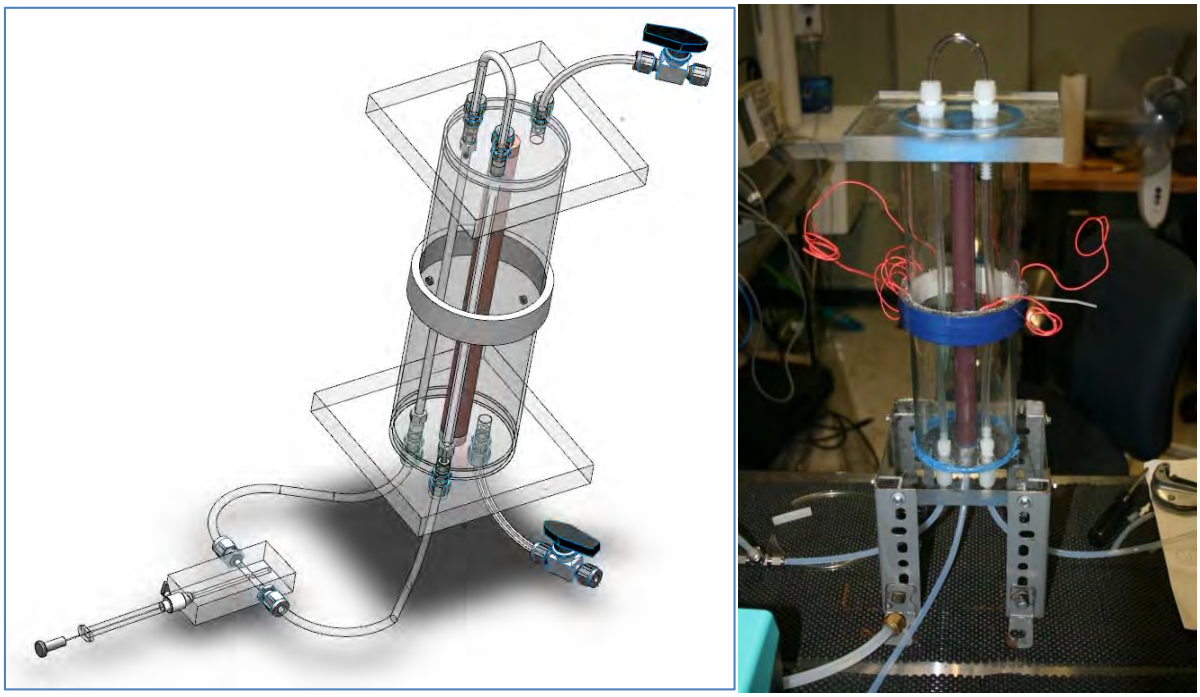

Figure 1. Left: Schematic of the 1st generation of simplified thigh with the bubble generation device. Right: As build 1st generation of simplified artificial thigh.

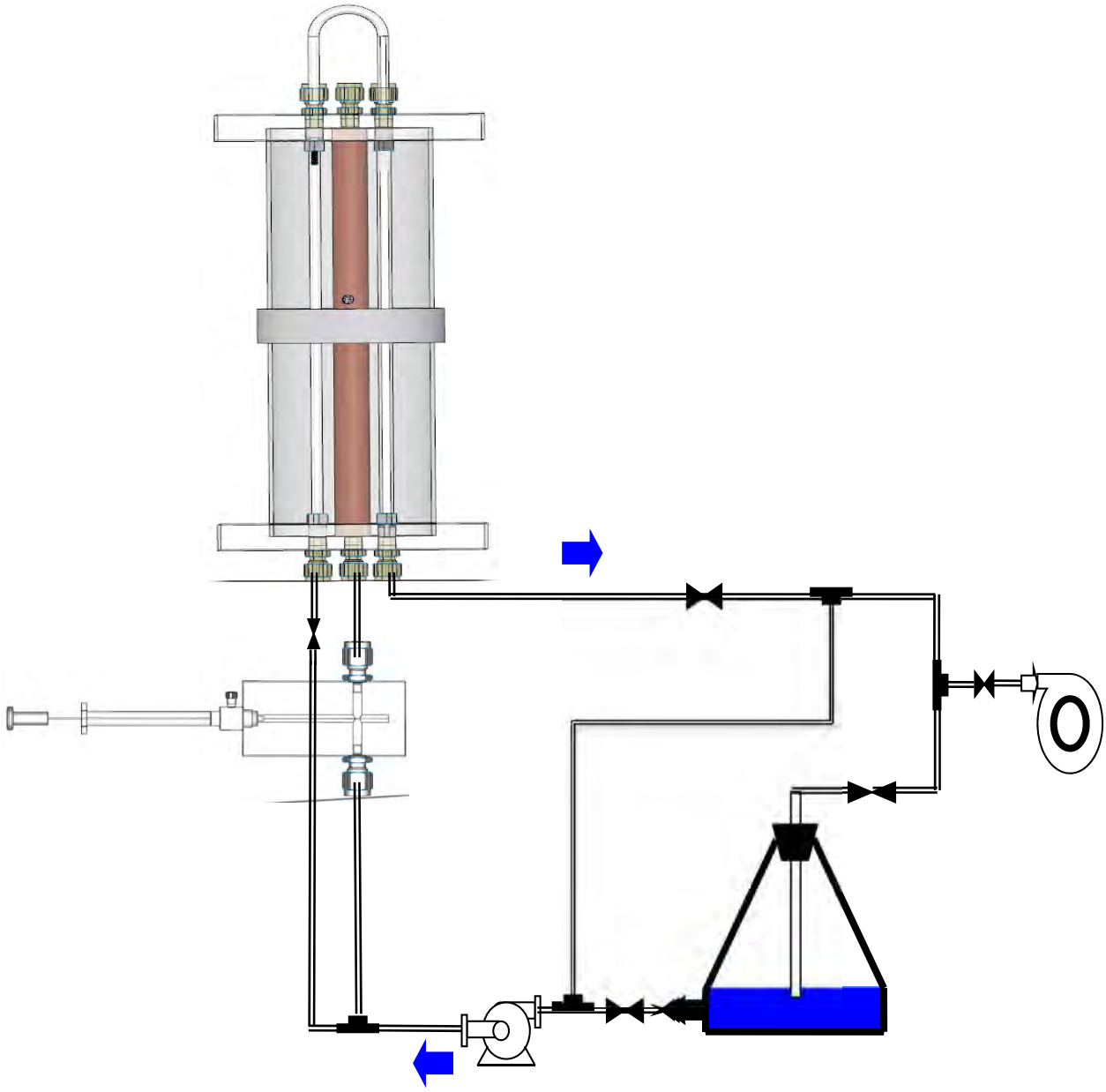

Figure 2. Experimental set-up. The artificial thigh and bubble generation system are connected to a filtering flask where water is degassed using a magnetic stirrer and vacuum pump. A peristaltic pump used for circulation inside the artery and vein is also shown.

3.1.2 2nd Generation of artificial thigh:

The second generation of artificial thigh was designed and constructed by the new graduate students that started to work on the project in the Fall semester 2012. The main difference with respect to generation one design, is that the bone is located in an off centered position, which is comparable with the location of the bone on an average human thigh. This change increases the complexity of the numerical simulations due to the loss of axial symmetry with respect to the

previous model. Additionally the new generation was designed to allow daily disassembling and assembling. This design and the results of the numerical simulations are well documented in the 3rd progress report submitted on September 2013. This new artificial thigh was significantly more robust that the first one. Some problems were observed due to the silicone used to glue the acrylic flanges. These problems are well documented in the 4th progress report submitted on September 2014. The disadvantage of this design, which was also something present in the first generation of artificial thigh is related to the bubble generation and the integration with the artificial thigh. Bubbles would get trapped at the fittings that were connecting the bubble generation device with the artificial thigh.

Figure 3. Experimental set-up

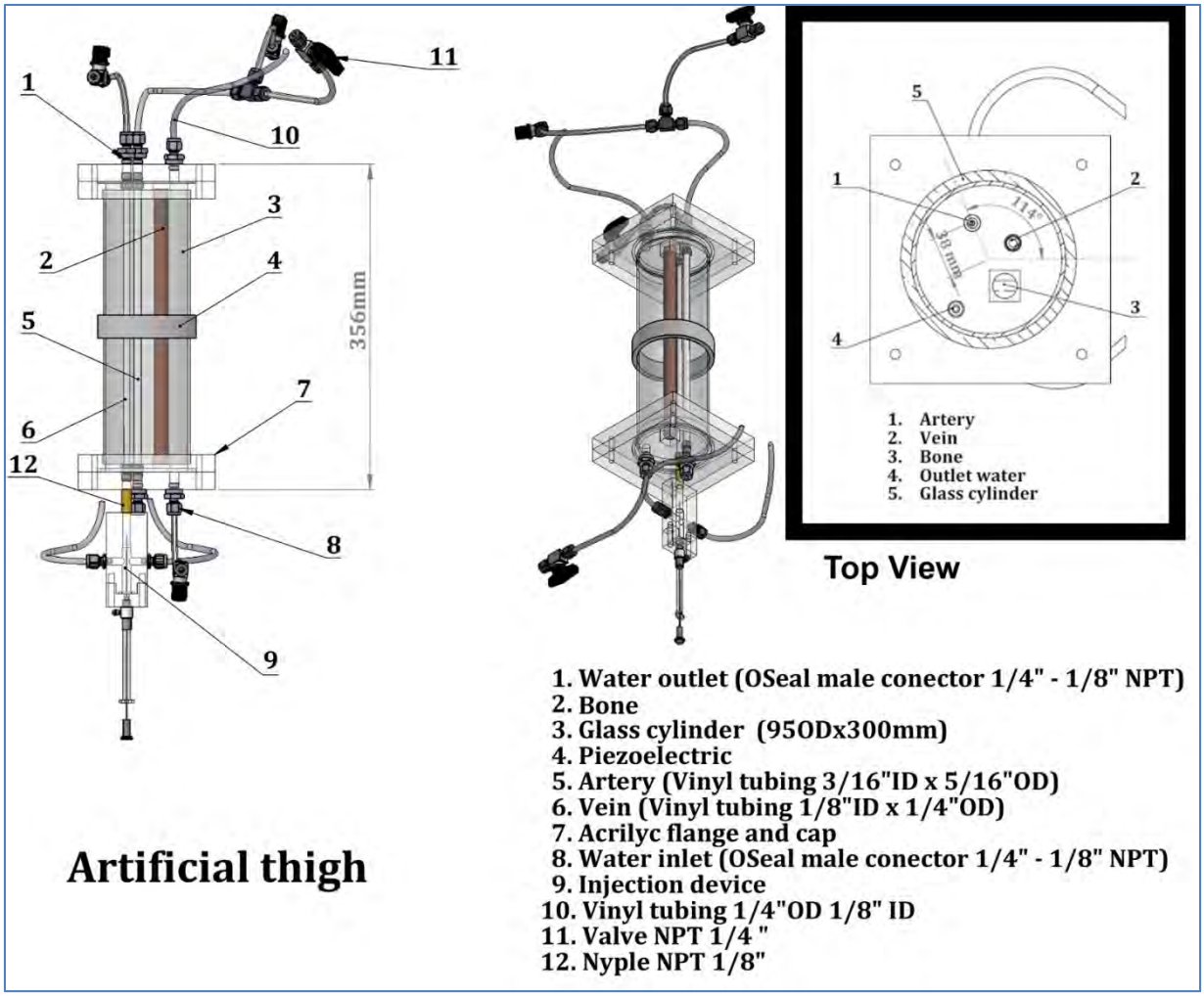

Figure 4. Solid-Works model of the 2nd Generation of the artificial thigh and the integrated bubble generation system.

3.1.3 3rd Generation of artificial thigh

The objective of the 3rd Generation of artificial thigh was to improve the integration with the bubble generation system.

New acrylic flanges were designed allowing for glass tubes to go through the acrylic flanges and connect to the artery and vein like vinyl tubes without the need of using metal fittings. The flanges were glued to the glass cylinder with clear silicone. Figure 5 shows the 2nd Generation and the 3rd Generation. Figure 6 shows a detailed schematic of the changes made to the acrylic flanges. This design has been proven robust, easy to disassemble and clean and capable of holding vacuum pressures up to 1Torr. Additionally the problems related to the accumulation of bubbles in the fittings was solved.

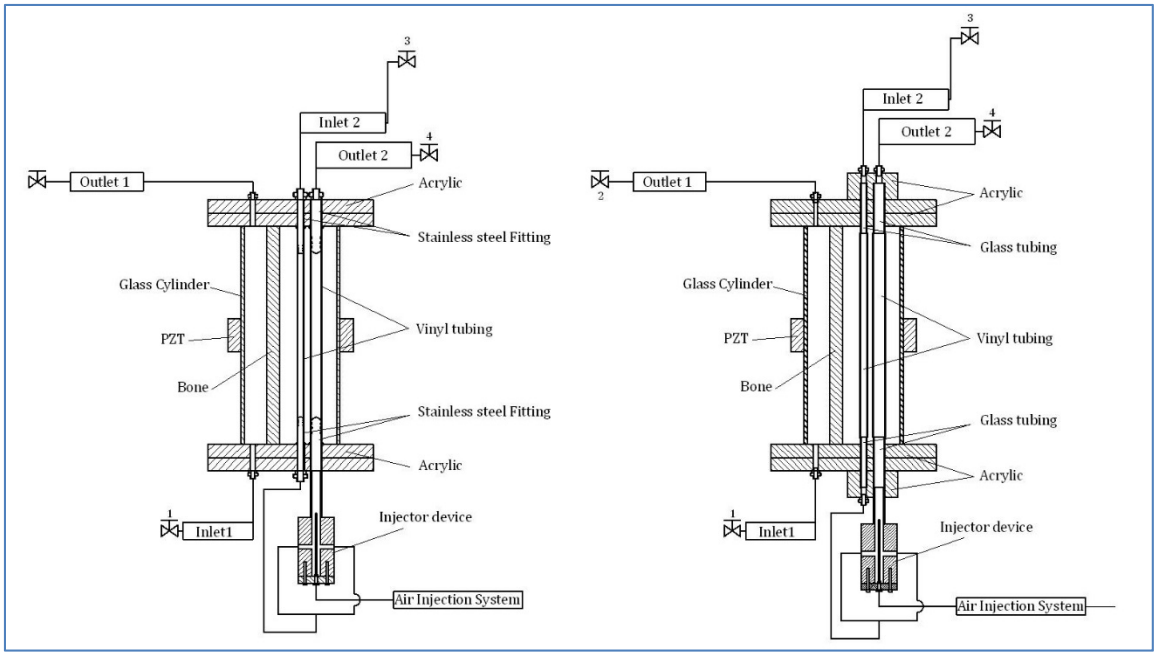

Figure 5. Left: 2nd Generation of artificial thigh. Right: 3rd Generation of artificial thigh

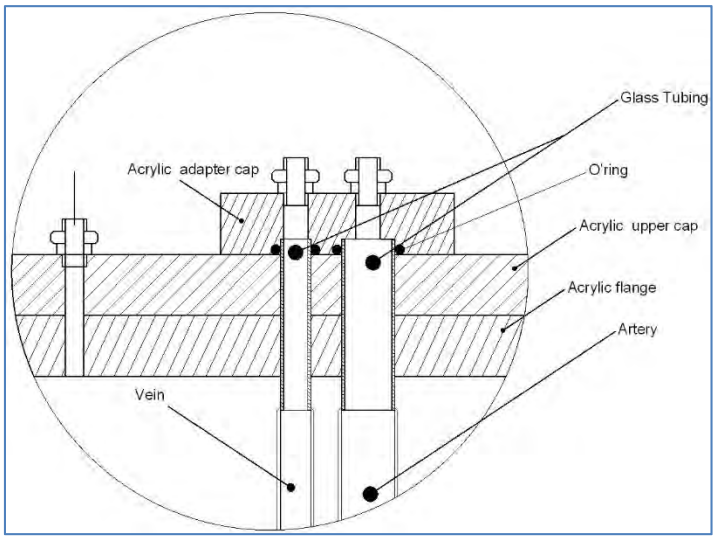

Figure 6. Detailed schematic of the modification made in the acrylic flanges in the 3rd Generation of artificial thigh.

3.2 Detailed work related to Task#4 and Task#5

3.2.1 First bubble generation device

The bubble generation device used for the measurements conducted with the 1st Generation of artificial thigh is shown in Figure 7. The integration with the artificial thigh is shown in Figure 1 (Left). As it can be observed from Figure 2, the system was originally thought to be with the syringe in the horizontal position and the flow in the vertical direction, such that the flow aids in the separation of the bubble produced at the tip of the needle. However, since the connection

between the bubble generation device and the artificial thigh was through flexible tubing, the bubbles were trapped and it was difficult to get them to move inside the artificial thigh. Therefore, a small modification was performed, in which the syringe was located in the vertical position and the flow coming from the vein in a direction perpendicular to the syringe would carry the bubble inside the artery like tube that was aligned with the syringe (see Figure 7. This design was used for the experiments conducted with the 1st generation of artificial thigh. Bubbles were generated and moved inside the artificial thigh but the bubble size was not controllable and bubbles were typically attached to the walls of the artery like tubes. This methodology was appropriate to determine the feasibility of the method however did not allowed us to conduct repeatable experiments and therefore it was not possible to obtain a correlation between electric signals and bubble size.

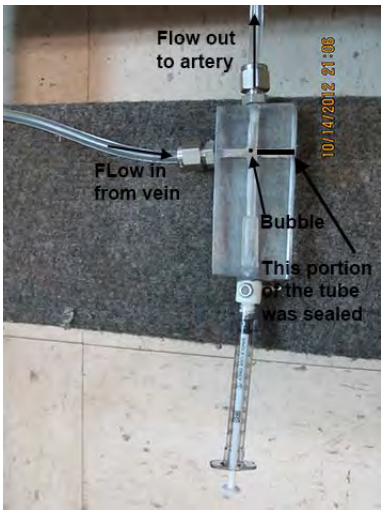

Figure 7. Image of the first bubble generation device constructed with the syringe located in the vertical direction.

3.2.2 Second bubble generation device

The second bubble generation device was developed with the 2nd Generation of artificial thigh. A detailed description was provided in the 3rd progress report submitted in September 2013, Figure 8 shows an image of the bubble generator device. This device was tested in three different configurations. All three methods deliver acceptable results with the third one being the best for creating smaller bubbles. The first method is described in detail in the 4th progress report submitted in September 2014, here a summary is provided. The second and third configurations were tested after the 4th progress report and are described in the present report.

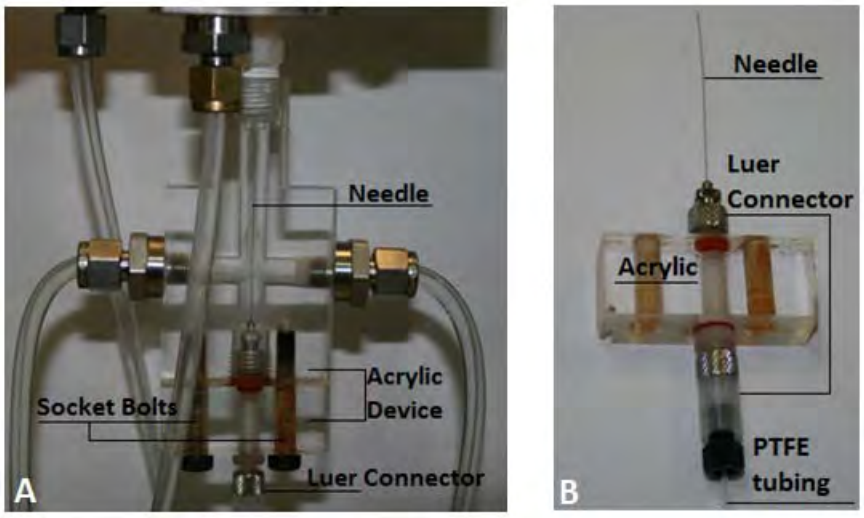

Figure 8. 2nd bubble generation device.

3.2.2.1 First configuration for bubble generation

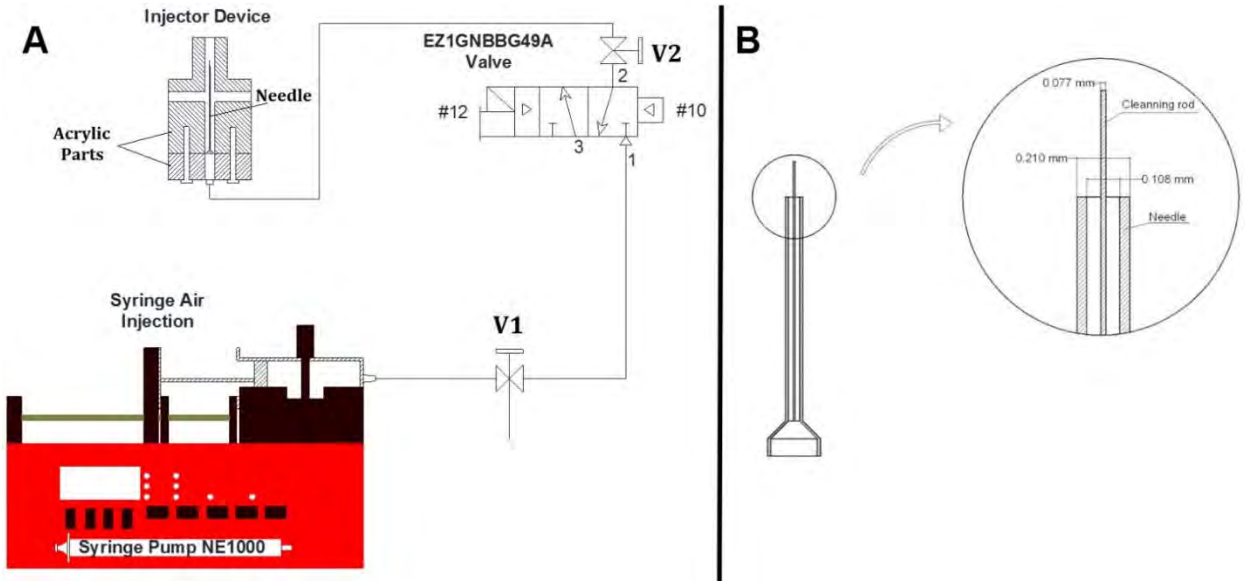

Figure 9. 1st configuration for bubble injection. (A) Complete system (B) Detail of the cleaning rod inside the gauge 33 needle

The first configuration is shown in Figure 9. The microbubbles are created injecting air into the artificial thigh. The syringe pump (NE1000, New Era Pump Systems, Farmingdale, NY) is used to regulate the initial volume of air inside a 20ml syringe and the volumetric flow rate, which is kept at 16ml/min. The syringe is connected to a valve and the injector device through a 22 gauge PTFE tubing. One electro-valve (single solenoid 3 way 1 position, normally closed) is used to control the duration of air injection for different initial volumes of air inside the syringe. A detail of the

LabView program used to control the solenoid valve is described in the 4th progress report submitted in September 2014.

In the 4th report submitted in September 2014, duration of air injection was kept at 20ms. This method always produces several bubbles, generally more than 4, sometimes 10 or 12, being the one with bigger diameter the one that enters the artificial thigh and approaches the PZT ring sooner, therefore being this bubble the one that is analyzed. It is desirable to produce just a few bubbles, otherwise there is a risk that bubbles might coalescence before entering the artificial thigh causing a bigger bubble to move along the artery-like tube. It was observed that by reducing the air injection time to 10ms between 1 and 4 bubbles were generally produced, therefore, this was the time used.

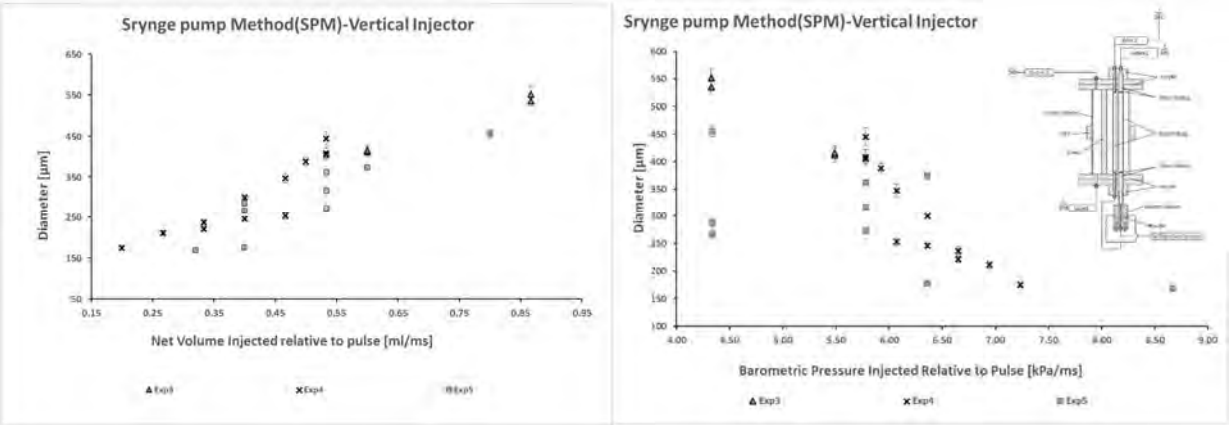

Figure 10. Left: Diameter of bubbles generated with the first configuration as a function of the net volume of air injected in 10ms. Right: The same data on the left but as a function of the injected pressure.

Figure 10 shows the results obtained with this configuration. The data shown in Figure 10 (Right) was obtained by measuring the pressure inside the 20ml syringe filled with different volumes with a pressure sensor (PXCPC-150GV, Omega Engineering, Stamford, CT), this was done to be able to compare the data with the 3rd configuration and it is important to note that this is the initial air pressure in the syringe.

The bubble size obtained with this method was more predictable, however, it was observed that with time the needles used were corroded and that a backpressure of the fluid was built against the needle was causing water to move inside the needle. The corrosion problem was verified by inspecting the needles with a microscope and comparing new needles, with needles that were new but in storage for more than 6 months and with needles that were used. The problem was detected in the new needles stored for long periods of time and the used ones. This issue was fixed by carefully cleaning needles after using then and by storing them in sealed packages. The backpressure problem is cause by the solenoid valve, when it closes and the issue is solved by changing the orientation of the needle to the horizontal position as described below.

3.2.2.2 *Second Configuration for bubble generation*

The second configuration has the injector device in the horizontal position (Figure 11). The rest of the method is like the one described for the first configuration. Figure 12 shows the results obtained with this configuration.

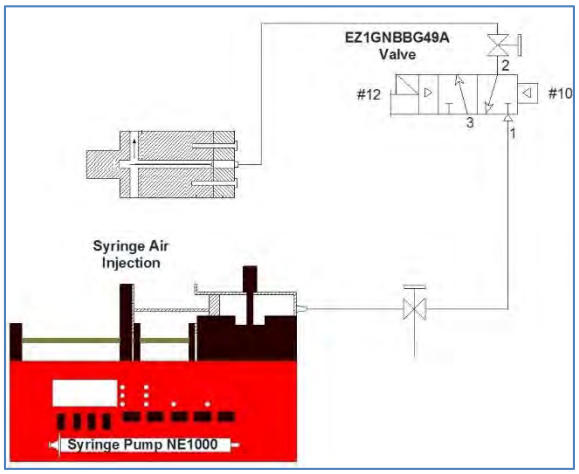

Figure 11. Second Configuration for bubble injection.

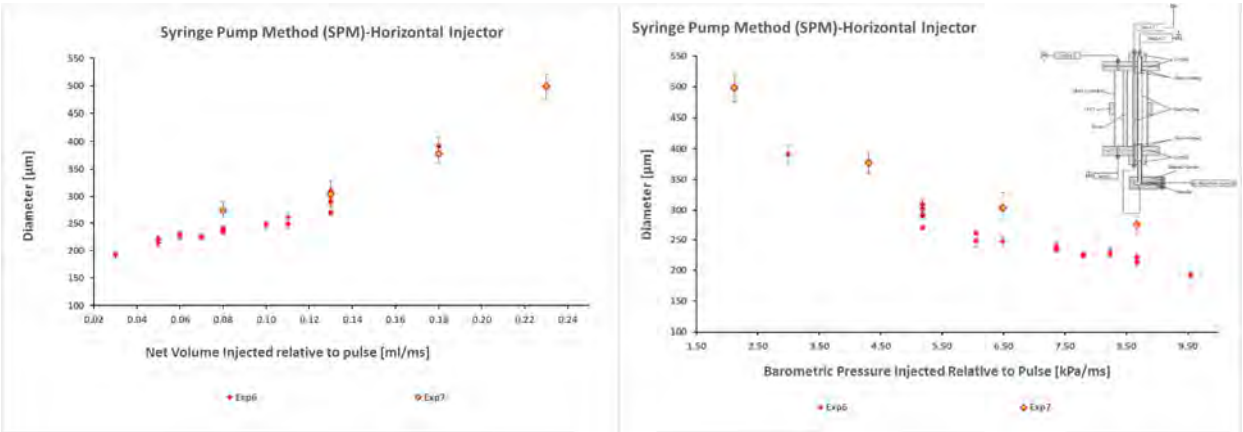

Figure 12. Left: Diameter of bubbles generated with the second configuration as a function of the net volume of air injected in 10ms. Right: The same data on the left but as a function of the injected pressure.

3.2.2.3 *Third configuration for bubble generation*

The third configuration uses a compressor (Craftsman air compressor 125psi) capable of controlling the pressure at the inlet of the solenoid valve instead of the syringe pump. A diagram of this configuration is shown in Figure 13. Based on the theoretical analysis on the bubble growth made by Prospereti and Hassan (1993) controlling the pressure gives a better control on the bubble growth at the tip of the needle. Results obtained with this configuration are shown in Figure 14 and provide the best results in term of bubble size control.

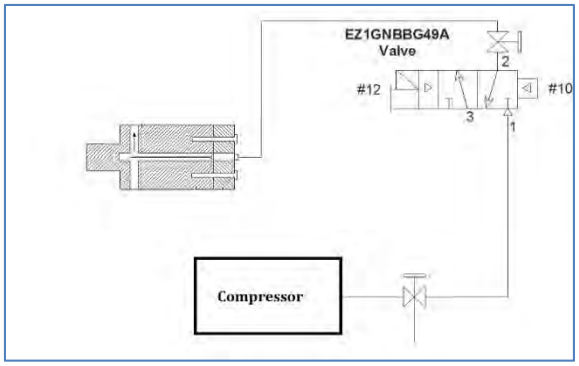

Figure 13. Diagram for the 3rd configuration for bubble generation

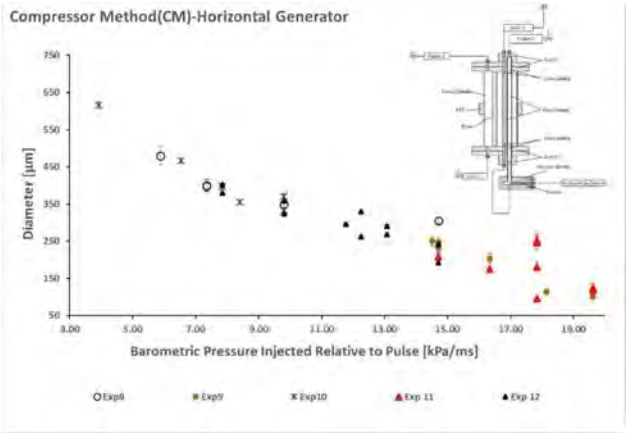

Figure 14. Diameter of bubbles generated with the third configuration as a function of the injected pressure for 10ms of the electro-valve aperture.

3.3 Detailed work related to Task#7

In order to obtain a correlation between bubble size and electric signals measured in the PZT it was necessary to be able to conduct repeatable experiments. This depends on several factors: (i) quality of experimental test section (ii) electronic noise (iii) water quality. The electronic noise was reduced by enclosing all electric circuits and replacing all the wires by grounded coaxial cables. The water quality was controlled by using distilled water filtered in the Millipore Simplicity 6000 water filtration system.

Two methods were tested. The first method was conducted with the 2nd generation of artificial thigh and the bubble generation device shown in Figure 8 but with a manual technique, using a 1ml syringe and injecting 0.4ml of air manually. These results were first reported in the 3rd progress report submitted in September 2013. The procedure is described in Section 3.3.1. The second method was conducted with the 3rd generation of artificial thigh and all three configurations for bubble generation. A description of this method is provided in Section 3.3.2.

3.3.1 Method 1

This method consisted in injecting a bubble in the artery while the PZT was turned off and by using fluid circulation. Once the bubble entered the artificial thigh, about 70mm above the bubble generation device, the PZT was turned on. A high speed camera was located close to the PZT ring to measure the bubble size just before crossing it. The bubble crossing the PZT was correlated with a decrease in the current measured in the PZT as shown in Figure 15. Figure 15 is obtained after applying the algorithm shown in Figure 16 to detect the amplitude peaks of each semi-cycle. Then, the algorithm shown in Figure 17 is used to determine the current drop. All the data obtained is shown in Figure 18 where the relative value in percentage is obtained as current drop divided the mean current value when no bubbles are present. The error is the standard deviation of the current when no bubble is present.

The bubbles were imaged in the artery just before entering the PZT

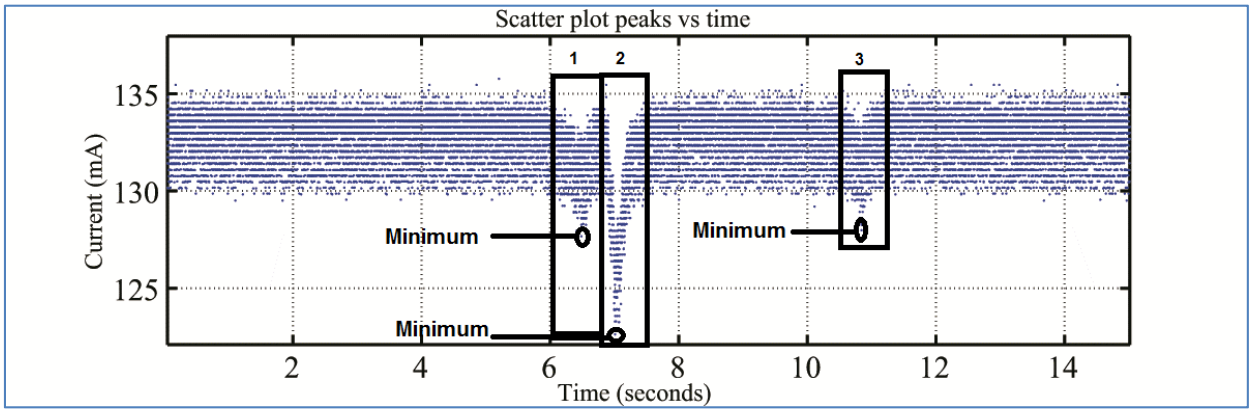

Figure 15. Sample signals of current drop in the PZT caused by the passage of a bubble.

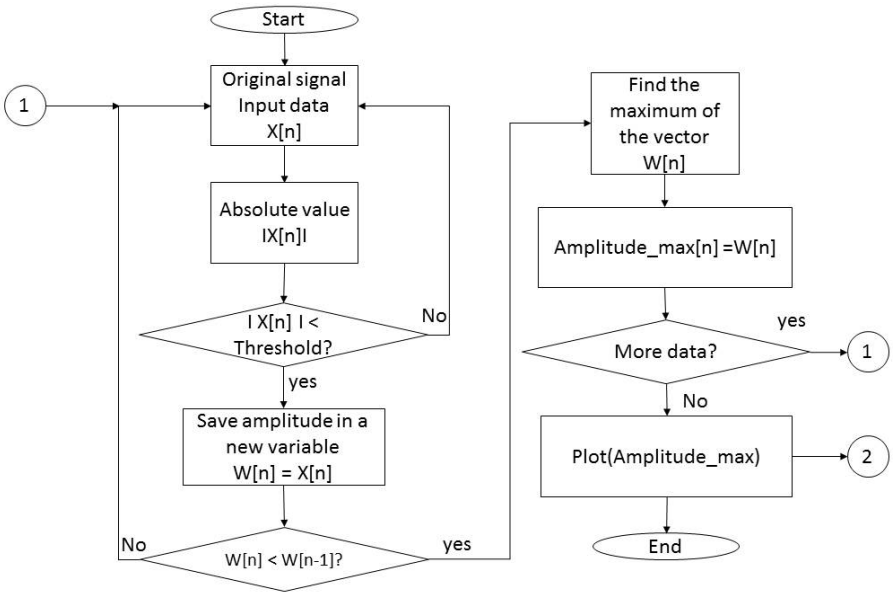

Figure 16: Block diagram for amplitude peaks detection. X(n) represents the original current signal acquired. The threshold value is used to improve the algorithm, a value of 80mA was used for the bubbles analyzed with method 1.

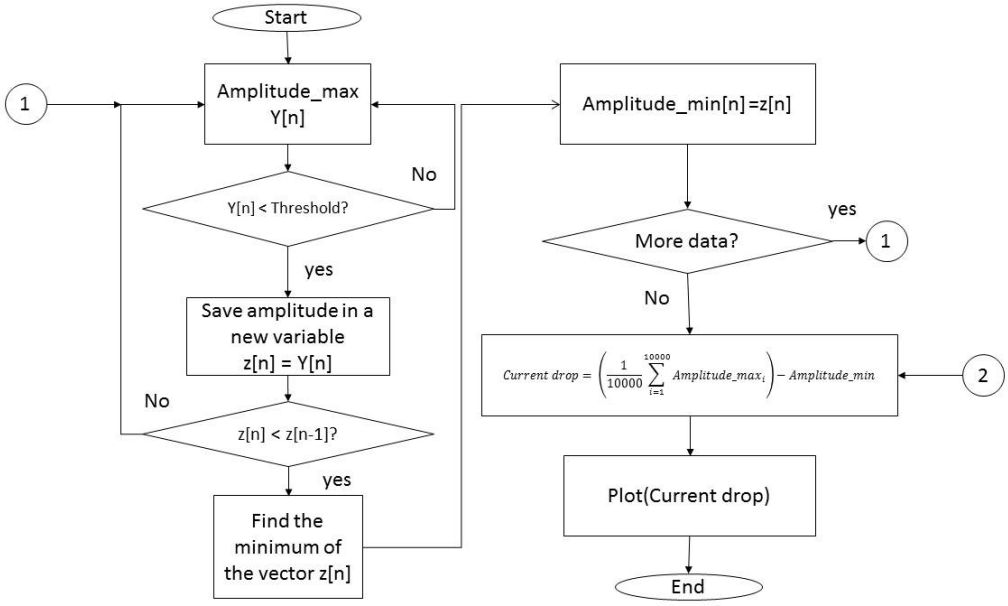

Figure 17: Block diagram for current drop detection. Y[n] are the data obtained after applying the algorithm of Figure 16 and the threshold is obtained by: threshold = $\overline{y(n)} - \sigma_{y(n)}$ with $\overline{y(n)}$ being the average value and $\sigma_{y(n)}$the standard deviation.

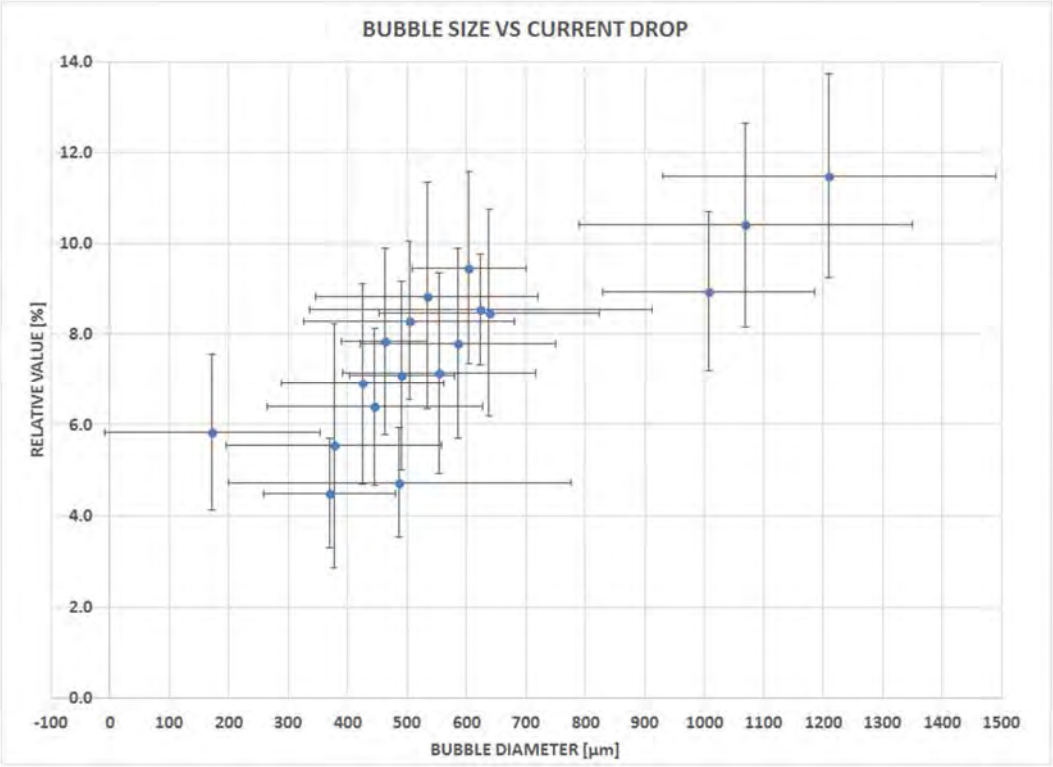

Figure 18: current drop with method 1. The water used in these experiments was only filtered by not distilled.

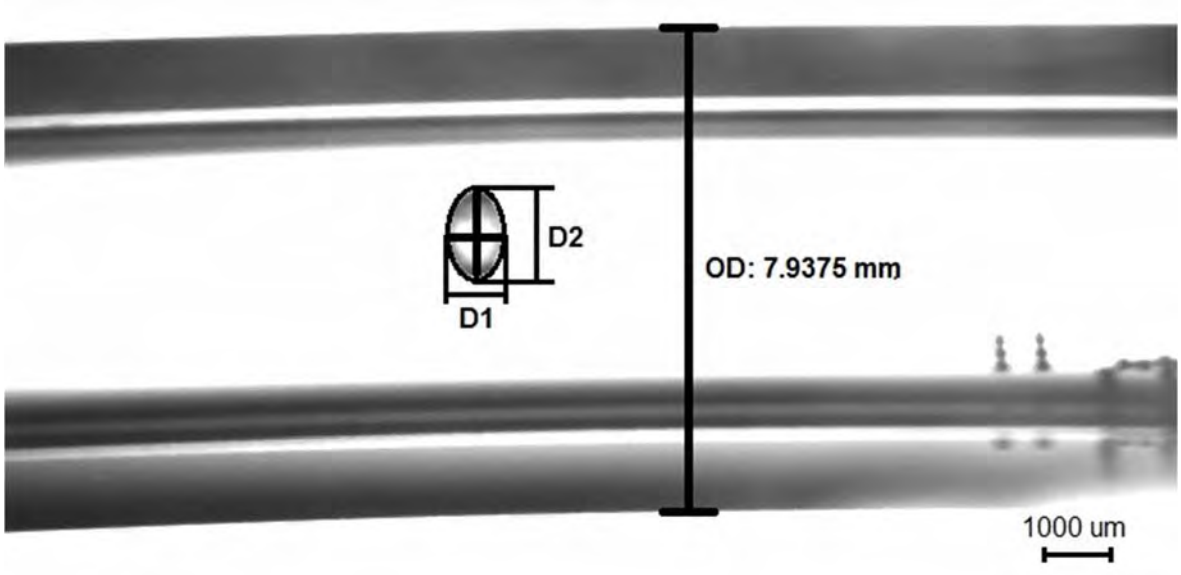

Figure 19: One bubble imaged in the artery during experiments conducted in 2013.

The diameter was obtained using three images of the same bubble. For each image the two diameters D1 and D2 were obtained and the average diameter was computed as $\overline{D_{average}} = \left(\frac{1}{6}\sum_{i=1}^{6} D_i\right)$ with an error of $\sigma = \sqrt{\frac{1}{(5)}\sum_{i=1}^{6}\left(D_i - \overline{D_{average}}\right)^2}$. The conversion between pixels from the image and actual size is done based on the artery outside diameter of 7.9375mm.

Since the PZT was turned on continuously, the bubbles smaller than 500μm in diameter were pushed towards the center of the cylinder, causing them to get attached to the walls of the artery-like tube where they would accumulate. This problem was overcome by using a transient method described below.

3.3.2 Method 2

In this method the PZT was actuated when the bubble was at specific places. Data was obtained actuating the PZT when bubbles were at its center, when bubbles were 1cm below the PZT and when bubbles were 2cm below the PZT. The bubbles were generated using the three different configurations described in sections 3.2.2.1 to 3.2.2.3. The 3rd generation of artificial thigh was used. The bubbles were imaged in the generation device and close to the PZT using two high speed cameras, however, the PZT was actuated based on visual observations. Because of the manual actuation of the PZT fluid circulation could not be applied. A total of

126 bubbles were measured when the PZT was actuated at the time the bubble was crossing its center. Of these 126 experiments 30 were done with water used as soft tissue, 18 were done with hyaluronic acid at 0.66% and the rest with hyaluronic acid at 1.05%. 38 experiments with hyaluronic acid at 1.05% included the additional measurements of 3 pill microphones located at the bottom border of the PZT, 1cm below and 2cm below.

25 bubbles were measured when the PZT was actuated when the bubble was 1cm below the bottom edge of the PZT and 20 bubbles were measured when the PZT was actuated when the bubble was 2cm below the bottom edge of the PZT.

The acoustic behavior of the artificial thigh with hyaluronic acid was similar to that of water. Details were reported in the 4th progress report submitted in September 2015, and the resonance frequency is maintain at 13148 ± 5 HZ.

Figure 20 shows all the data obtained with this method.

In order to obtain the relative value plot in Figure 20 it is first necessary to obtain a reference signal when the PZT is actuated and there are no bubbles in the system. A typical reference signal is showed in Figure 21. From this signal the root mean square value is computed for the first 10000 data points equivalent to 10msec according to the following equation:

$$Root\ mean\ square = \sqrt{\frac{1}{N}\sum_{i=1}^{N} x_i^2}$$

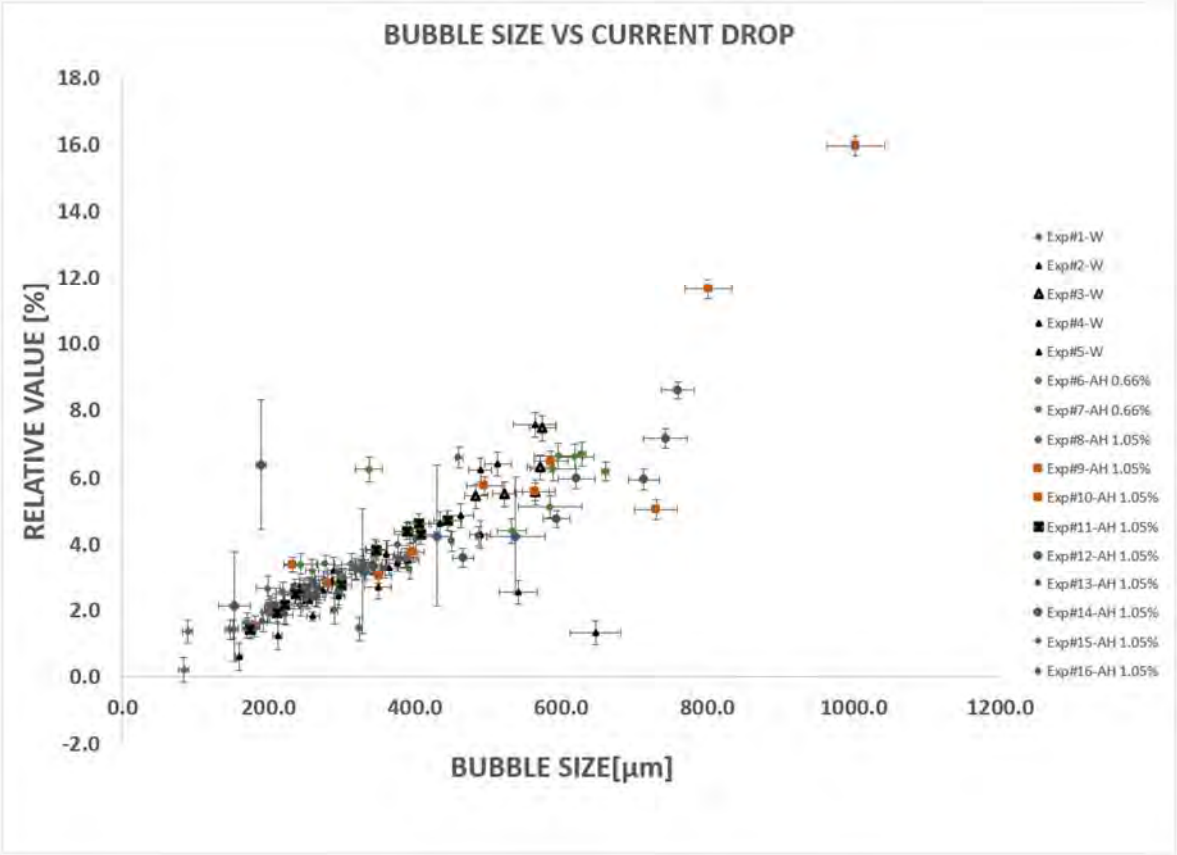

Figure 20. Effect of bubble size measured in the PZT when it is actuated at the time the bubble reaches the PZT center. The error bars were computed based on the DAQ card precision and the error propagation of the relative value of the difference in root mean square.

When the bubble is at the center of the PZT the PZT is actuated and one sample signal of the current measured in PZT is showed in Figure 22. The root mean square of this signal is also computed and the relative value plot in Figure 20 is obtained from:

$$Relative\ value = \frac{\left(\sqrt{\frac{1}{N}\sum_{i=1}^{N} y_i^2} - \sqrt{\frac{1}{N}\sum_{i=1}^{N} x_i^2}\right)}{\sqrt{\frac{1}{N}\sum_{i=1}^{N} x_i^2}} * 100$$

Where x represents the data without bubble and y the data with bubble.

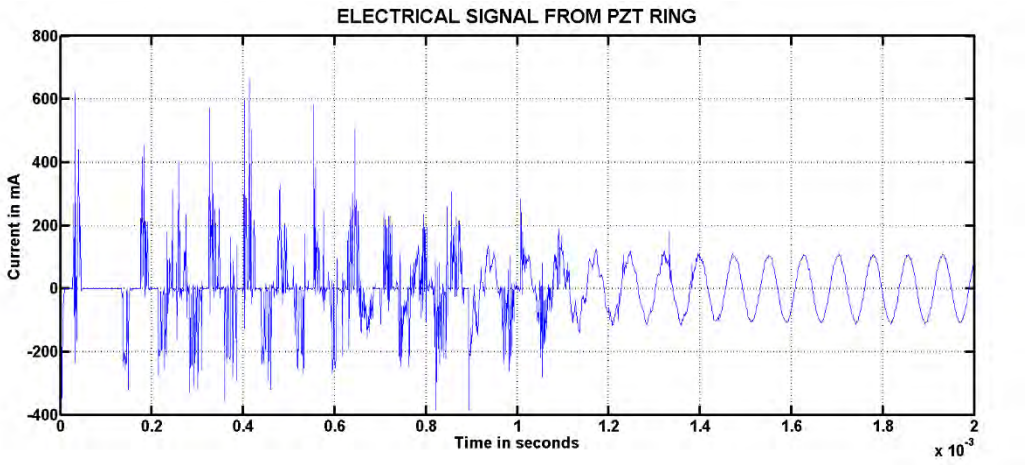

Figure 21: Electrical signal without bubble.

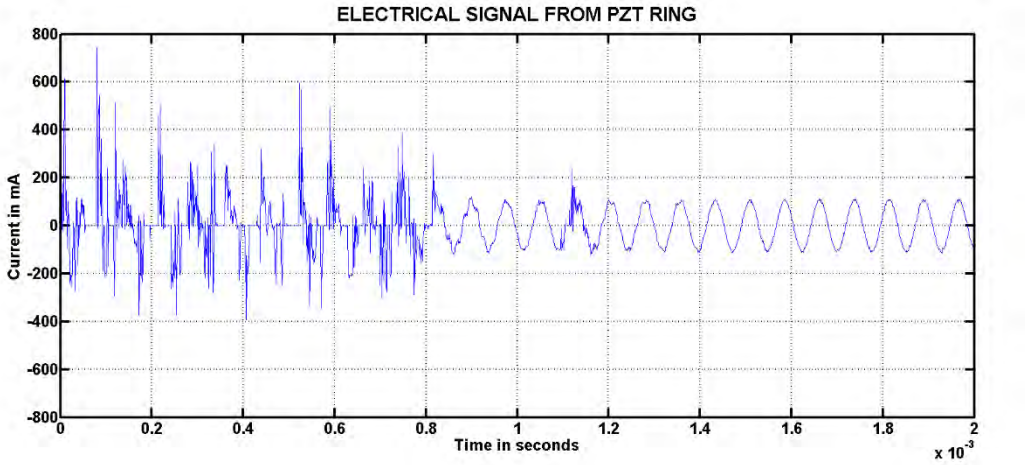

Figure 22: Electrical signal with bubble

Figure 23 shows the results when the PZT was actuated when the bubble was at 1cm from the PZT and Figure 24 shows the results when the PZT is actuated when the bubble is 2cm away from the PZT. From the data in Figure 24 it can be concluded that if bubbles are further away than 2cm from the PZT, the system cannot detect them, however if they are at 1cm a smaller signal is measured, therefore, a big bubble located 1cm away from the PZT when the PZT is actuated could be confused with a smaller bubble crossing the PZT center. In order to solve this issue the voltage from pill microphones located at the PZT border (see Figure 25), at 1cm from the PZT (see Figure 26) and 2cm from the PZT (see Figure 27) was acquired simultaneously with the current measured on the PZT.

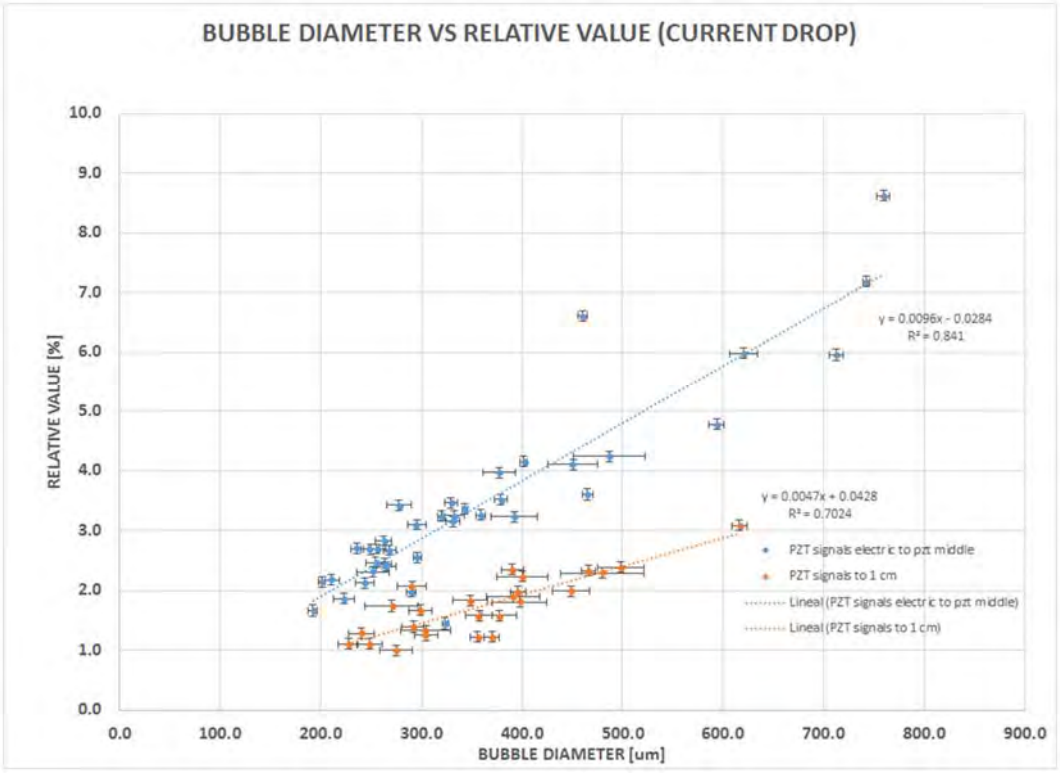

Figure 23. Comparison of data obtained when the PZT was actuated when the bubble was at the PZT center with data obtained when the PZT was actuated when the bubble was at 1cm from the PZT.

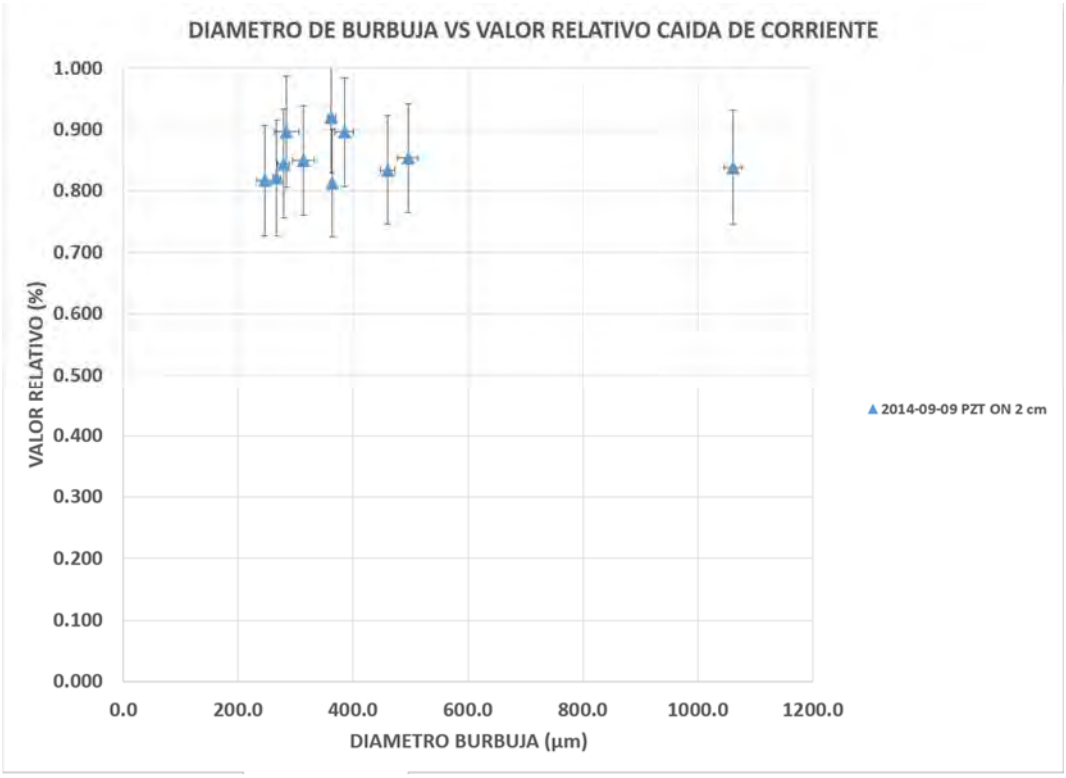

Figure 24. Data obtained when the PZT was actuated when the bubble was at 2cm below the PZT.

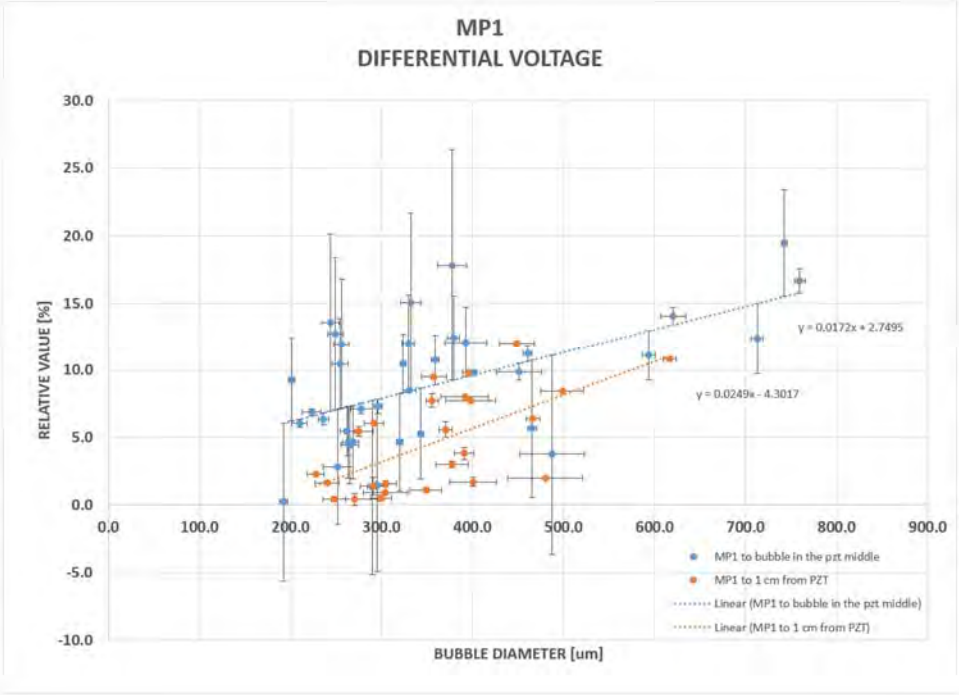

Figure 25. Data obtained measuring the voltage in a pill microphone locate at the bottom edge of the PZT when the PZT was actuated when the bubble reached the PZT center (blue data points) and when the PZT was actuated when the bubble was at 1cm from the PZT (orange data points)

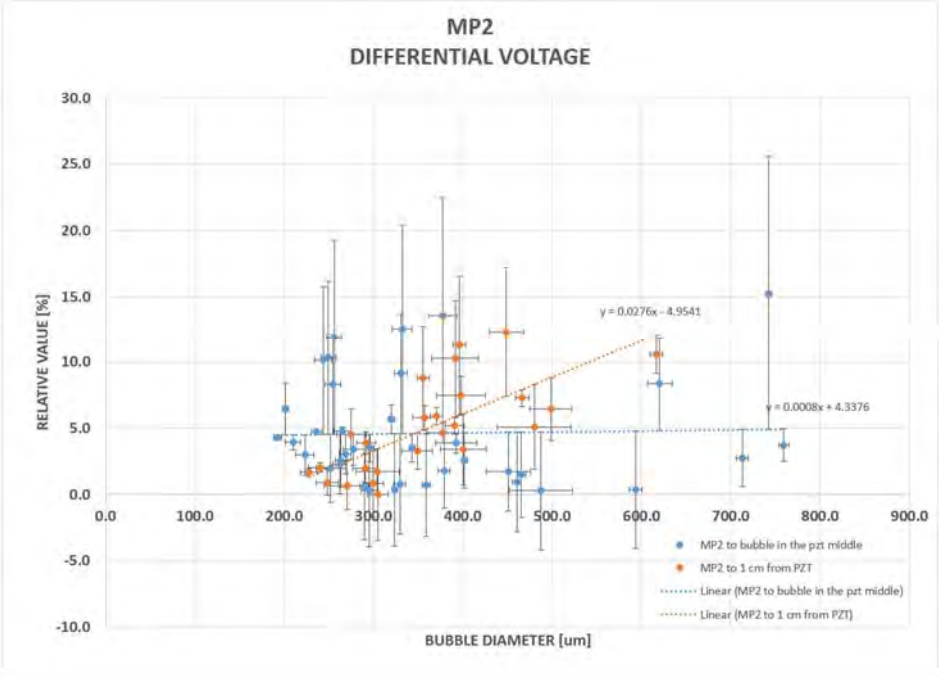

Figure 26. Data obtained measuring the voltage in a pill microphone located at 1cm from the bottom edge of the PZT when the PZT was actuated when the bubble reached the PZT center (blue data points) and when the PZT was actuated when the bubble was at 1cm from the PZT (orange data points)

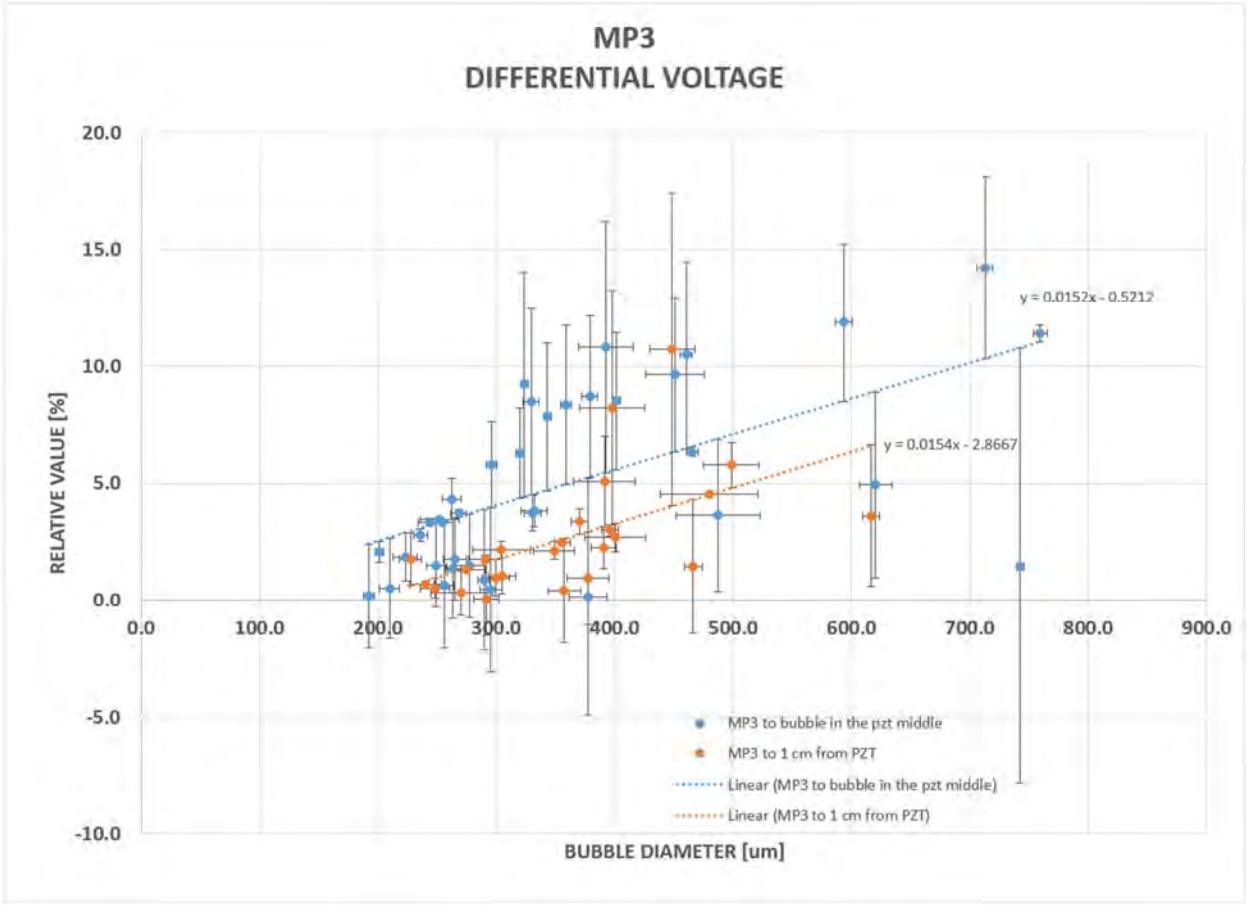

Figure 27. Data obtained measuring the voltage in a pill microphone located 2cm from the bottom edge of the PZT when the PZT was actuated when the bubble reached the PZT center (blue data points) and when the PZT was actuated when the bubble was at 1cm from the PZT (orange data points)

3.4 Detailed work related to Task#10

A total of 7 experiment were performed by adding the bubbles inside the soft tissue medium. For this purpose a long needle gauge 33 was used. Once the bubble is generated it moves vertically towards the PZT, however, since the hyaluronic acid is more viscous than water, it took longer for the bubble to reach the PZT, therefore, we used the Bjerknes forces to move the bubble closer to the PZT. When the bubble was 5mm below the PZT the electronic equipment was turned off. The PZT was actuated when the bubble reached the PZT center. Figure 28 shows a schematic diagram of the generation technique and Figure 29 shows the results. As with the case of bubbles generated in the artery-like tube the system is capable of detecting and sizing the bubbles.

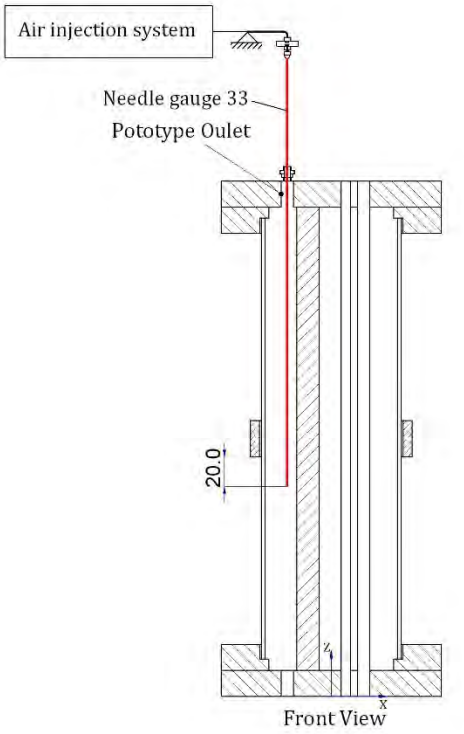

Figure 28. Location of the needle used to create bubbles in the hyaluronic acid at 20mm below the PZT

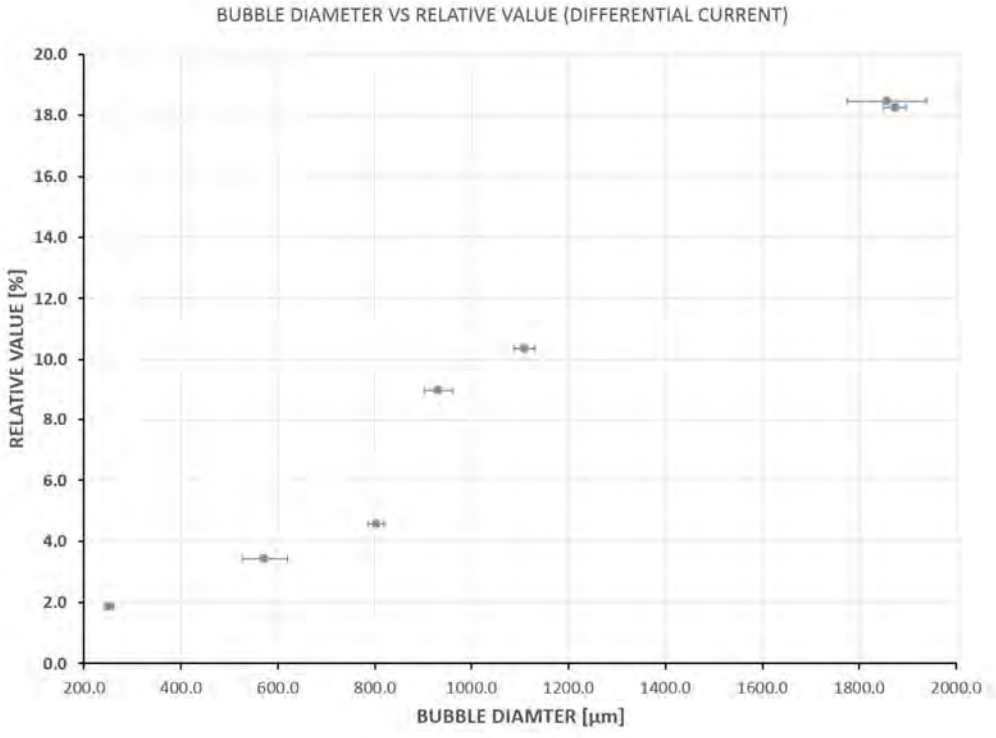

Figure 29. Signal obtained with the current measured on the PZT when the PZT was actuated at the time the bubble reached the PZT center.

3.5 Detailed work related to Task#11

The final objective of the project is to be able to determine the size of bubbles based on measured electric signals on the PZT and pill microphones. For this purpose the three different algorithms described in the 4th Progress report submitted in September 2014 were tested. The k-mean, the SVM and the neural network. Three different analysis were performed to determine the effectivity of the different algorithms in predicting the bubble size after being trained.

The first analysis was performed with 100 data points corresponding the PZT actuated when the bubbles were crossing the PZT center. The data introduced to train the algorithms was bubble size and relative difference of the root mean square in the current signal. Then only the current information was introduced to determine their effectivity at predicting bubble size. The results are shown in Figure 30 and Table 1 for the k-mean, in Figure 31 and Table 2 for the SVM and in Figure 32 and Table 3 for the neural network. The accuracy being 84%, 89% and 91% respectively.

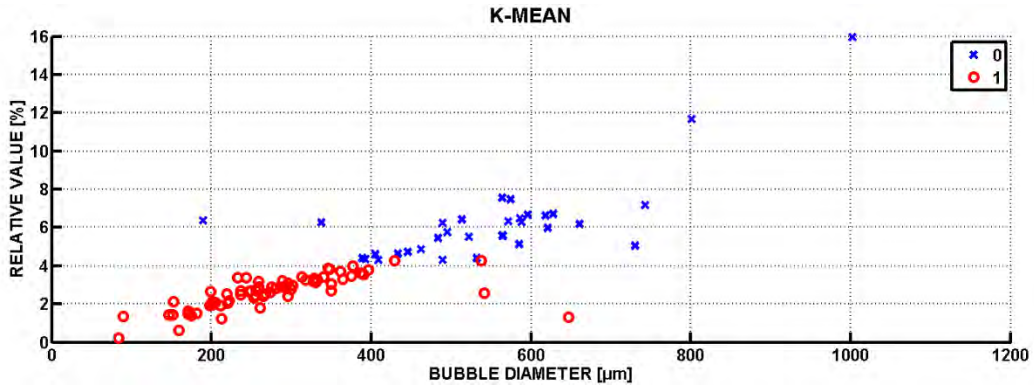

Figure 30. Prediction of the k-mean algorithm when 100 data corresponding to the PZT being actuated when the bubbles were at its center was used. "0" represents bubbles predicted to have a size smaller than 500 µm and "1" represents bubbles bigger than 500 µm.

		Real		
		Menor	Mayor	Total
k-mean	Menor	64	3	67
	Mayor	13	20	33
	Total	77	23	100

Table 1. Confusion matrix for the k-mean algorithm. Accuracy 84%

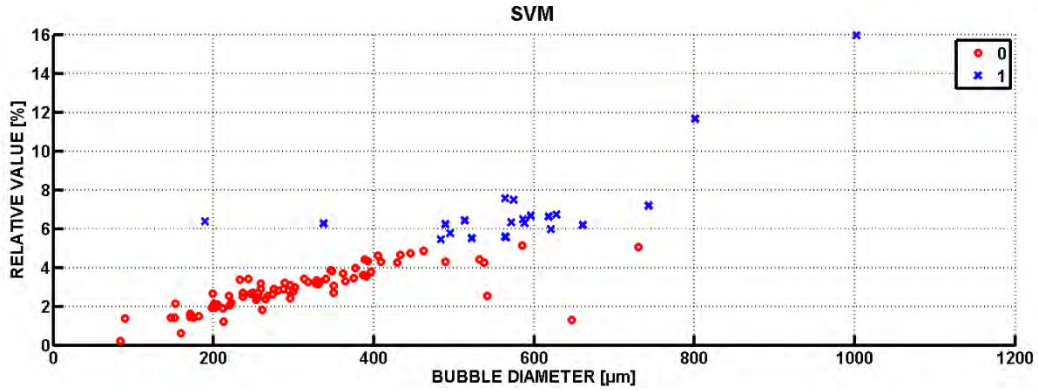

Figure 31. Results of the SVM algorithm when 100 data corresponding to the PZT being actuated when the bubbles were at its center was used. "0" represents bubbles predicted to have a size smaller than 500 µm and "1" represents bubbles bigger than 500 µm.

		Real		
		Menor	Mayor	Total
SVM	Menor	72	6	78
	Mayor	5	17	22
	Total	77	23	100

Table 2. Confusion matrix for the SVM algorithm. Accuracy 89%

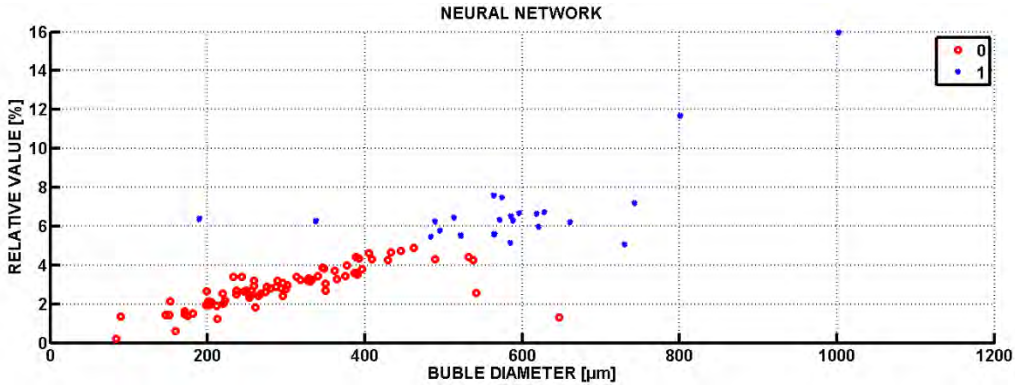

Figure 32. Results of the Neural network algorithm when 100 data corresponding to the PZT being actuated when the bubbles were at its center was used. "0" represents bubbles predicted to have a size smaller than 500 µm and "1" represents bubbles bigger than 500 µm.

		Real		
		Menor	Mayor	Total
NN	Menor	72	4	76

	Mayor	5	19	24
	Total	77	23	100

Table 3. Confusion matrix for the neural network algorithm. Accuracy 91%

The performance of the algorithms was also analyzed for the case in which 4 characteristic were introduced in the classifiers: (i) current in the PZT (ii) voltage in pill microphone 1 (iii) voltage in pill microphone 2 and (iv) voltage in pill microphone 3. First only the 38 data points corresponding to the PZT being actuated when the bubbles were at the PZT center were analyzed. The results are shown in Table 4, Table 5 and Table 6.

		Real		
		Menor	Mayor	Total
k-mean	Menor	24	1	25
	Mayor	1	12	13
	Total	25	13	38

Table 4. Confusion matrix for the k-mean algorithm with 4 features for the data points corresponding to the PZT actuated when the bubbles were at the center of the PZT. The accuracy is 95%.

		Real		
		Menor	Mayor	Total
SVM	Menor	22	1	23
	Mayor	1	14	15
	Total	23	15	38

Table 5. Confusion matrix for the SVM algorithm with 4 features for the data points corresponding to the PZT actuated when the bubbles were at the center of the PZT. The accuracy is 95%

		Real		
		Menor	Mayor	Total
NN	Menor	23	1	24
	Mayor	0	14	14
	Total	23	15	38

Table 6. Confusion matrix for the neural network algorithm with 4 features for the data points corresponding to the PZT actuated when the bubbles were at the center of the PZT. The accuracy is 97%

The last and most important test was done using the data corresponding to the PZT actuated when the bubbles were at the PZT center and when the bubbles were 1cm below the PZT. The objective is to determine if the system will be able to correctly determine the bubble size measuring current in the PZT and voltage in 3 pill microphones.

Assuming the sensor works in a pulsated manner, and bubbles are present in the blood stream, then if the bubbles moving along the artery are further away than 2cm from the PZT the system will not detect them. If the bubble are between 0-1cm from the PZT the system will detect them.

The question is: Will our sensor be able to distinguish a small bubble that might be at the center of the PZT when the PZT is actuated from a big bubble that is at 1cm from the PZT when the PZT is actuated? Based on the obtained results, the answer to that question, is Yes it will. The results are shown in Table 7, Table 8 and Table 9.

		Real		
		Menor	Mayor	Total
k-mean	Menor	33	3	36
	Mayor	2	25	27
	Total	35	28	63

Table 7. Confusion matrix for the k-mean algorithm with 4 features for the data points corresponding to the PZT actuated when the bubbles were at the center of the PZT and for bubbles that were at 1cm away from the PZT when it was actuated. The accuracy is 92%

		Real		
		Menor	Mayor	Total
SVM	Menor	31	10	41
	Mayor	4	18	22
	Total	35	28	63

Table 8. Confusion matrix for the SVM algorithm with 4 features for the data points corresponding to the PZT actuated when the bubbles were at the center of the PZT and for bubbles that were at 1cm away from the PZT when it was actuated. The accuracy is 78%

		Real		
		Menor	Mayor	Total
NN	Menor	33	1	34
	Mayor	2	27	29
	Total	35	28	63

Table 9. Confusion matrix for the neural network algorithm with 4 features for the data points corresponding to the PZT actuated when the bubbles were at the center of the PZT and for bubbles that were at 1cm away from the PZT when it was actuated. The accuracy is 95%.

Even though the neural network and the k-mean were almost equally effective it is expected that the k-mean will performed worse than neural network when more than two classes are considered. This statement is based on the performance of the classifiers alone when the 100 data corresponding to the PZT actuated when the bubble was at the PZT center for the case of 2 groups vs 5 groups. The k-mean method had an accuracy of 92% for the case of 2 groups, decreasing it accuracy to 88% when 5 groups are used. The neural network had an accuracy of 100% when 2 groups were used and it only decreased to 98% when 5 groups were used.

4 Bibliography

Prosperetti A. and Oguz Hasan N. Dynamics of bubble growth and detachment from a needle. J. Fluid Mech. 1993. Vol 257 pp 111-145